Heliyon 9 (2023) e20295

Contents lists available at ScienceDirect

Heliyon

journal homepage: www.cell.com/heliyon

An exploratory research on antitumor effect of drug-eluting slow-releasing electrospinning membranes

Li Li [a,1], Feng Li [b,1], Zhifeng Zhao [c,1], Rongli Xie [d], Dan Xu [e], Min Ding [e], Jun Zhang [e], Dongjie Shen [d,**], Jian Fei [e,*]

[a] Department of Otolaryngology-Head and Neck Surgery, Xijing Hospital, Air Force Medical University, Xi'an, Shaanxi Province, China
[b] Department of Emergency, Shanghai Jiao Tong University Affiliated Sixth People's Hospital, Shanghai, China
[c] Xijing Hospital of Digestive Diseases, Air Force Military Medical University, Xi'an, Shaanxi Province, China
[d] Department of General Surgery, Ruijin Hospital Luwan Branch, Affiliated to Shanghai Jiao Tong University, Shanghai, China
[e] Department of General Surgery, Ruijin Hospital, Affiliated to Shanghai Jiao Tong University, Shanghai, China

ARTICLE INFO

Keywords:
Drug eluting membrane
Electrospinning
PTX
Malignant obstructive jaundice

ABSTRACT

Objective: To evaluate the long-term inhibition of malignant biliary tumor growth using paclitaxel (PTX)-covered polycaprolactone (PCL) electrospun membranes.
Methods: A mixture of PCL, a material used to fabricate polymer stents, and PTX, a widely used chemotherapeutic agent, was synthesized by electrospinning. After preparing the drug-eluting membrane, drug release and fiber degradation were assessed *in vitro* under different pH conditions. The QBC939 cholangiocarcinoma cell line was cultured to establish a xenograft nude mouse model. Finally, the drug-eluting membrane was implanted into the mouse model, and the relative tumor inhibition rate was evaluated.
Results: A new PTX-loaded PCL electrospun fiber membrane was developed. The drug release rate was about 20–40% in the 32-day release cycle, and the release quantity was between 20 and 170 mg. As pH decreased, the release rate increased significantly. The degradation rate of the fiber membranes *in vitro* was approximately 20–48%, and was positively correlated with the drug loading rate. In animal experiments, the growth of tumors in mice was suppressed using drug-eluting membranes.
Conclusion: The PTX-loaded PCL electrospun fiber membrane enhanced the long-term drug release and exhibited excellent antitumor effects *in vivo*.

1. Introduction

Malignant obstructive jaundice (MOJ) has recently been associated with various malignant and benign conditions, including hepatomas, pancreatic cancer, cholangiocarcinoma, gallbladder cancer, and malignant lymphadenopathy. Rarely, it also occurs in benign conditions, such as choledocholithiasis, chronic pancreatitis, and postoperative strictures. Owing to limitations in diagnostic techniques, fewer than 20% of patients with distal or hilar malignant strictures are candidates for curative resection because they are

* Corresponding author. No. 197, Second Ruijin Road, Huangpu District, Shanghai, PR China.
** Corresponding author. No. 149, South Chongqing Road, Huangpu District, Shanghai, PR China.
E-mail addresses: eastheroshen@163.com (D. Shen), fj10777@rjh.com.cn (J. Fei).
[1] LL, FL and ZZ contributed equally.

https://doi.org/10.1016/j.heliyon.2023.e20295
Received 13 June 2023; Received in revised form 18 September 2023; Accepted 18 September 2023
Available online 20 September 2023

poor surgical candidates or have unresectable diseases secondary to local spread and distant metastases [1]. Biliary obstruction develops in 70–90% of these patients, resulting in jaundice, cholangitis, pruritus, malabsorption, coagulopathy, and hepatocellular dysfunction. Therefore, most patients require palliative therapies, including percutaneous transhepatic cholangial drainage (PTCD) [2] and endoscopic retrograde cholangiopancreatography (ERCP). Polymer and self-expandable metal stents (SEMS) are commonly used for bile expansion and drainage [3]. However, stents can become occluded over time due to tumor ingrowth or overgrowth, mucosal hyperplasia, biliary sludge, and food impaction, hindering patient recovery. To avoid restenosis, drug-eluting stents (DESs) have emerged as a new treatment option for MOJ [4–7]. Electrospinning, a well-established strategy for constructing fibrous membranes used for tissue regeneration [8] and loading functional agents [9], has been employed to develop functionalized membranes capable of delivering therapeutic agents, and polycaprolactone (PCL)-based nanofibers are one of the most popularly used materials in electrospinning applications [10].

This study aimed to develop a new nanofiber membrane that can cover bile stents, especially in terms of practicability and long-term effects. It refers to a versatile stent that can mechanically expand the bile tract and serve as a carrier for local drug delivery with its unique design and material. We fabricated polymer membranes made of a mixture of paclitaxel (PTX) and PCL by electrospinning, which enabled the fibers to be fine enough to reach nanometer-scale dimensions with good biocompatibility.

2. Methods

2.1. Materials

The analytical grade chemical reagents were used as received without further purification. PCL was provided by the Institute of Traumatology and Orthopaedics, Ruijin Hospital, affiliated with Shanghai Jiao Tong University School of Medicine. The experimental protocol was established according to the ethical guidelines of the Helsinki Declaration and was approved by the Ethics Committee of Ruijin Hospital affiliated with Shanghai Jiao Tong University (SYXK [SHANGHAI 2018–0027]).

2.2. Electrospinning

A PTX-loaded membrane consisting of PCL nanofibers was prepared by electrospinning under the following conditions: a voltage of 14 kV, flow rate of 0.04 mL/min, and receiving distance of 15 cm. This fiber membrane can be used to cover the metal stent. The drug-eluting membrane was provided by our laboratory at the Institute of Traumatology and Orthopaedics, Ruijin Hospital, affiliated with Shanghai Jiao Tong University School of Medicine. Four kinds of membranes were prepared using the fabrication method described above for examination with varying PCL concentrations of 0%, 0.5%, 1%, and 2%.

2.3. Characterizations

The morphology of drug-eluting membranes were examined using scanning electron microscopy (SEM, FEI Quanta 200, Netherlands). The sizes and thicknesses of the fibers were measured using a micrometer. The surface wettability of the fiber stents was evaluated by measuring the water contact angles (WCA) using a Kruss GmbH DSA 100 Mk 2 goniometer (Hamburg, Germany). The average diameters of the different drug-eluting fibers were measured using the ImageTool software.

2.4. In vitro drug release

To evaluate the *in vitro* release behavior of PTX, a mass of 20.0 mg of drug-eluting PCL fibrous scaffolds containing 0.5%, 1%, and 2% drug and non-drug-eluting PCL fibers were immersed in 25 mL of 154 mM phosphate-buffered saline (PBS, pH 7.4) and 25 mL acetate-acetate buffer solution (pH 4.0). Each fibrous membrane in the buffer solution consisted of three parallel specimens. The suspension was shaken at a speed of 100 rpm in a shaking water bath at 37 °C for 48 h. At each time node, 1.0 mL of the buffer was removed for analysis, and 1.0 mL of fresh buffer was added to the rest of the incubation. The PTX release was measured using an ultraviolet spectrophotometer (UV–vis; UNICAM, UV300, Thermo Spectronic, USA).

2.5. In vitro membrane degradation

The process of fiber degradation was evaluated based on the mass loss of the fibrous scaffolds. As mentioned above, accurately pre-weighed drug-eluting membranes were divided into three groups according to PTX gradient concentrations. The specimens were rinsed and dried to a constant weight at each time node. The remaining dry weight was compared with the initial weight. The fibers underwent floating, suspension, and precipitation for ten weeks during this period. Therefore, the mass losses of the fibrous scaffolds were measured.

2.6. In vitro QBC939 culture

The human cholangiocarcinoma cell line (QBC939), which was prepared to mimic the *in vivo* environment of a biliary malignant tumor (BMT), was provided by the Institute of Surgical Research, Ruijin Hospital Affiliated to Shanghai Jiao Tong University School of Medicine (Shanghai, China). The cell lines were cultured in DMEM with 10% fetal bovine serum (FBS, Sigma, U.S.A.) and 1% double-

antibody in a humidified incubator at 37 °C with 5% CO_2. The culture medium was replaced every two days. Once QBC939s reached 80–90% confluence, they would be passed at a 1:2 ratio. As a result, a total of 1.56×10^8 QBC939s were prepared for tumor xenografts.

2.7. Tumor xenograft and treatment

A total of 112 female 4-week-old SPF C56BL/6 mice were purchased from the Shanghai Cancer Institute for subcutaneous xenografts and 1.4×10^6 QBC939 cells were suspended in 200 μL culture medium and injected subcutaneously into the right sub-axillary region of the mice. The volumes were calculated using the following formula: $0.5 \times \text{length} \times \text{width}^2$. When the tumor volume reached 62.5 mm^3, the mice were divided into five groups: control (group A), blank membrane (group B), intraperitoneal injection chemotherapy (group C), 2% PTX-loaded fibrous membrane (group D), and chemotherapy with 2% PTX-loaded fibrous membrane (group E). Each group consisted of 21 mice divided into three subgroups. During the 4-week experiment, PTX was injected weekly into groups C and E at a 10 mg/kg dose. Over that time, 2% PTX-loaded fibrous scaffolds, with a 4 g/kg dosage, were implanted surgically upon the tumor in groups D and E. After recovery from the anesthesia, the mice were returned to their cages.

2.8. Anticancer effect analysis

The entire experiment lasted for three weeks. At the end of each week, a subgroup of the mice was sacrificed. Tumor volume was measured.

2.9. Statistical analysis

Data are presented as mean ± standard deviation (SD). Significance testing was performed using a one-way analysis of variance (ANOVA), followed by Bonferroni's post hoc test. $^*p < 0.05$, $^{**}p < 0.01$, and $^{***}p < 0.001$ were considered statistically significant. After *in vivo* experiments, we calculated the tumor volume (TV), relative tumor volume (RTV), and relative tumor proliferation rate (T/C). If the T/C value was more than 60%, it was considered invalid; however, if the value was below 60% and there was a statistical difference between the groups, we considered the result to be persuasive and valid. RTV=Vt/V0 (V0: tumor volume on day 0; Vt: tumor volume after every week of measurement). T/C = TRTV/CRTV × 100% (TRTV: RTV of the treatment group; CRTV: RTV of the control group).

3. Results

3.1. Standard PTX-releasing in vitro

The PTX-mixed membranes were placed in a standard solution (PBS), and the elution concentration was monitored for the curve. The correlation coefficient R^2 was 0.99996. The line chart suggests that the linear relationship was strong when PTX range was 0.5–30 μg/mL (Fig. 1).

3.2. PTX-releasing curve in pH 7.4 solution

The first experiment was the nanofibers drug release in a solution of pH 7.4 to imitate normal tissue internal environment. It can be concluded that in the first five days, the drug release presented a burst effect. Approximately 10–25% of the quantity was released in the groups (Fig. 2). The follow-up release process was milder and more extensive. The drug release rates were also distinct for different drug-loading rates of the stents. The greater the amount of drug loaded into the membranes, the higher the rate of drug release during

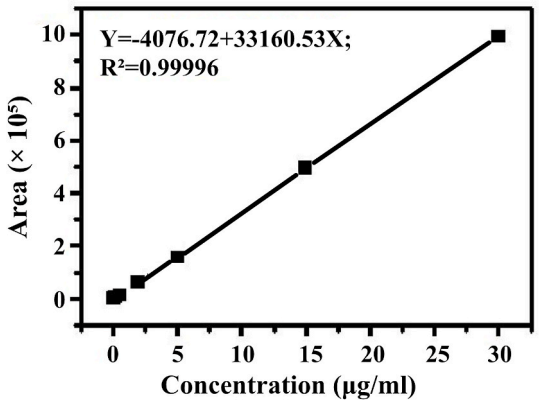

Fig. 1. Concentration-area line chart.

the experiment, which fluctuated between 17 and 40%. When the drug-load rate was 1.0%, the drug-release rates between the electrospun nanofibrous membrane and the flux film were similar at approximately 25%. Consequently, the total drug release increased as the drug concentration increased (Fig. 3).

3.3. PTX-releasing curve in pH 4.0 solution

As the experiment above imitates the internal environment of humans, the experiment below imitates the environment of the human biliary tract, where the pH is approximately 4.0. The burst effect in the first five days is similar in Figs. 4 and 3. However, the release rates were higher than those in pH 7.4 and could attain approximately 30–40%. The follow-up release process was milder and more extensive. The greater the amount of drug loaded into the membranes, the higher the drug release rate during the experiment, which fluctuated from 55 to 73%. When the concentration reached the maximum of 2.0%, the release rate reached the maximum of 73% among the four groups. When the drug loading rate was 1.0%, the drug release rate of the electrospun nanofibrous membrane was higher than that of the flux film ($p < 0.05$). As the drug loading rate increased, the drug release rate also increased. Consequently, the disparity in the total drug release between the different groups was greater (Fig. 5). The maximum amount released was approximately 320 μg.

3.4. Study on the degradation of PTX-loading membranes in vitro

The drug-loaded nanofibers were placed in PBS for ten weeks for the *in vitro* membrane degradation experiment. Weight loss and molecular weight change curves of the different drug-loaded fiber membranes are shown in Fig. 6b and c, respectively. As seen from the figure, the weight loss of the fiber gradually increased as drug loading increased. The maximum weight loss observed was 48%. The molecular weight reduction of the fibers was less than 28%, indicating the performance of a typical surface degradation model.

3.5. The drug-eluting membrane reduced the growth of xenografted tumors in nude mice

The mice were divided into five groups: control, blank membrane, chemotherapy, 2% PTX membrane, and chemotherapy with 2% PTX membrane. Tumor volumes at the beginning and end of the experiments were calculated separately. The results indicated a significant decrease in tumor volume of the chemotherapy and 2% membrane groups (Table 1; Fig. 7).

Fig. 7 illustrates that treatment in Groups C, D, and E yields favorable effects in reducing tumor volume, thereby highlighting the anti-tumor properties of the drug-loaded fibrous membranes. Remarkably, Group E exhibited the lowest tumor volume on both days 14 and 21, suggesting that the addition of local chemotherapy to systemic chemotherapy exerts a stronger inhibitory effect on tumor growth. This outcome can be attributed to a higher local drug concentration achieved through the dual drug delivery pathways rather than administration via a single route.

Groups C and E exhibited further decreases in tumor volume on day 14, while Group D experienced a slight rebound. Notably, the tumor volume in Group E remained lower than that in Group C. These findings suggest that the drug-loaded fibrous membrane continues to release drugs between days 14 and 21, exerting a certain inhibitory effect on tumor growth. However, the diminishing inhibitory effect may be attributed to insufficient local drug concentration within the tumor.

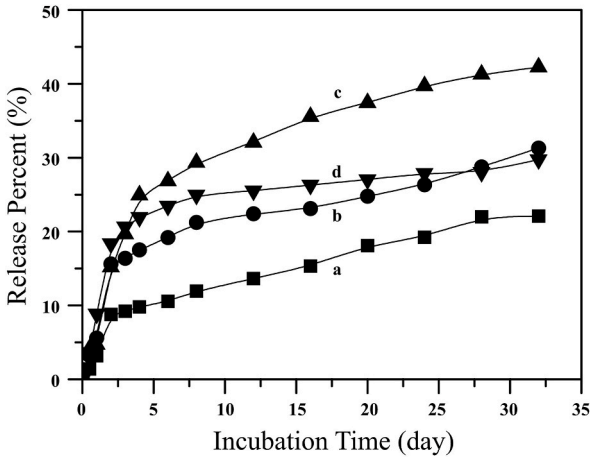

Fig. 2. Relationship between PTX release percentage and incubation time in pH 7.4 solution. There were four kinds of groups. Group A was PCL-0.5-fiber (■), whose concentration was 0.5%. Group B, whose concentration was 1.0%, was marked as PCL-1.0-fiber (●). Group C was marked as PCL-2.0-fiber (▲). Group D was a traditional flux film membrane PCL-1.0-film (▼) used as the control group.

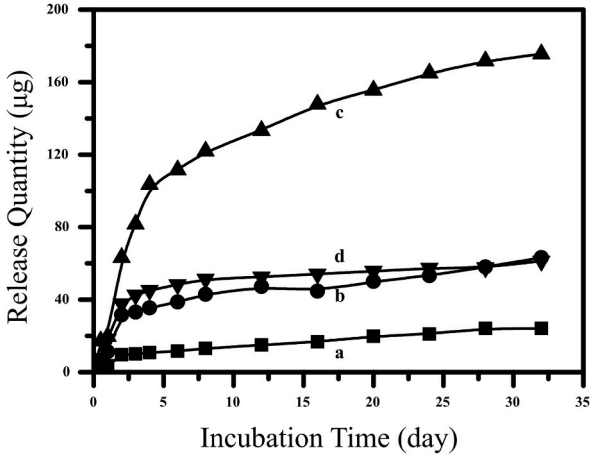

Fig. 3. Cumulative drug release of PTX-mixed membrane (net weight: 20 mg) in the pH 7.4 solution. The four groups were the same as in the figure above. They were respectively PCL-0.5-fiber (■), PCL-1.0-fiber (●), PCL-2.0-fiber (▲), PCL-1.0-film (▼).

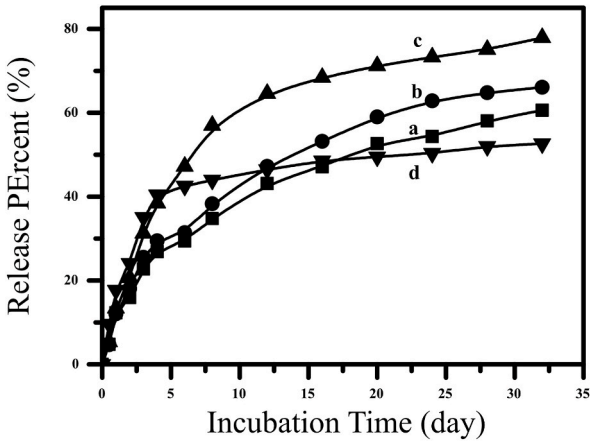

Fig. 4. Relationship between PTX release percentage and incubation time in pH 4.0 solution. There were four groups: group A. PCL-0.5-fiber (■), B. PCL-1.0-fiber (●), C. PCL-2.0-fiber (▲), D. PCL-1.0-film (▼).

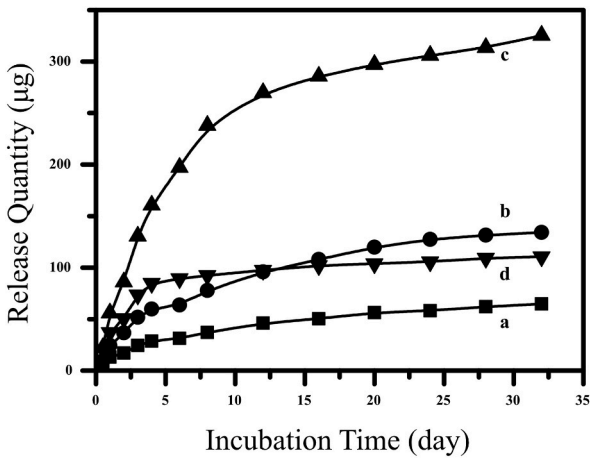

Fig. 5. Cumulative drug release of PTX-mixed membrane (net weight: 20 mg) in pH 4.0 solution. The four groups were group A. PCL-0.5-fiber (■), group B. PCL-1.0-fiber (●), group C. PCL-2.0-fiber (▲), group D. PCL-1.0-film (▼).

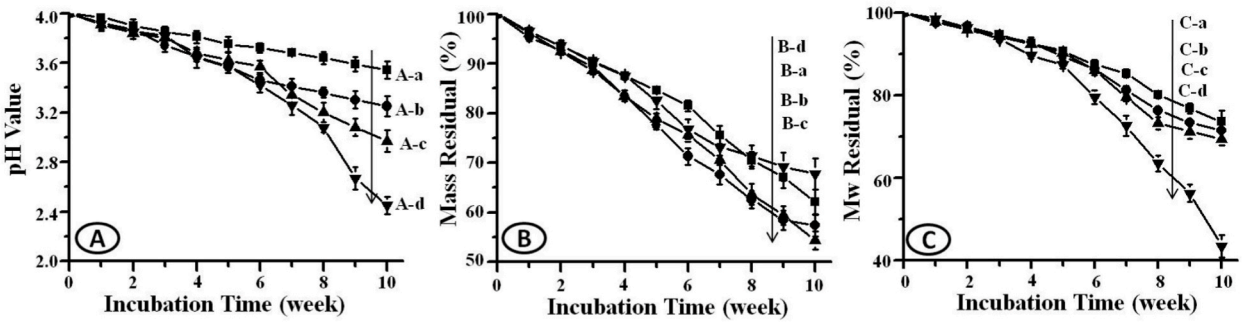

Fig. 6. aRelationship between incubation time and pH value
Fig. 6bRelationship between incubation time and mass residual
Fig. 6cRelationship between incubation time and molecular weight (Mw) residual.

Table 1
Influence on cholangiocarcinoma-xenograft nude mice (QBC939) after different treatments.

Group	TV (mm^3)			RTV		T/C (%)	
	day 0	day 14	day 21	day 14	day 21	day 14	day 21
A	62.5	1012.1 ± 466.7	1854.7 ± 582.7	16.19 ± 7.45	29.68 ± 8.07	/	/
B	62.5	657.3 ± 454.6	/	9.72 ± 4.27	/	60.1	/
C	62.5	146 ± 80.8	177.3 ± 85.7	2.34 ± 1.29*	2.83 ± 1.37*	14.4	9.5
D	62.5	97.2 ± 51.3	209.4 ± 112.5	1.56 ± 0.82*	3.35 ± 1.80*	9.6	11.2
E	62.5	77.4 ± 37.3	138.7 ± 69.7	1.36 ± 1.00**	2.62 ± 1.31**	8.4	8.8

Group A represents the control group. The mice were fed regularly. Group B was the blank membrane group. Mice were implanted with blank membranes that did not carry PTX, and Group C was the intraperitoneal injection chemotherapy group. Mice received PTX solution, (concentration of 1 mg/mL) injected into the abdomen every week; Group D was the 2% PTX-loaded fibrous membrane group. Mice were implanted with fixed PTX-mixed membranes (2% PTX) under their dorsal skin; mice in group E received PTX solution, (concentration as 1 mg/mL) injected into the abdomen every week as in group C, and PTX-mixed membranes (2% PTX) were implanted and fixed under their dorsal skin membranes as in group D.
Compared with group A, *$P < 0.05$, **$P < 0.01$.
Group E compared with groups C and D, $P < 0.05$.

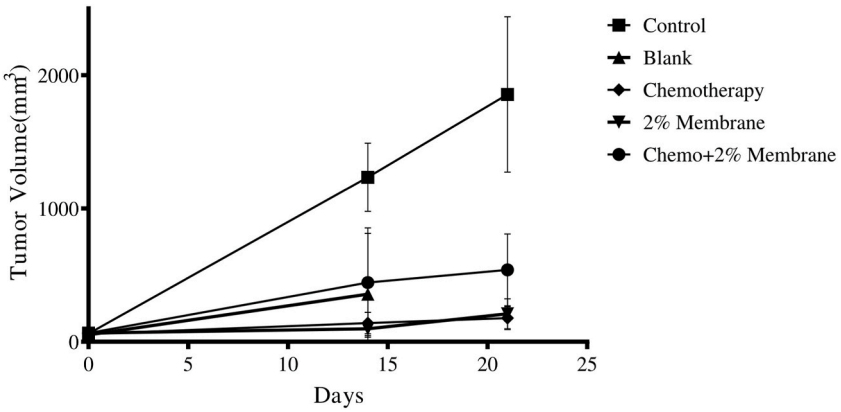

Fig. 7. Tumor volumes in different groups of cholangiocarcinoma-bearing mice (QBC939). The five groups were distinctively: control group (■), blank membrane group (▲), chemotherapy group (◆), 2% PTX membrane group (▼), and chemotherapy with 2% PTX membrane group (●).

4. Discussion

Malignant obstructive jaundice is particularly difficult to treat. In recent years, the incidence and mortality rates of this disease have significantly increased, attracting widespread attention worldwide. Among the principal treatment options including surgical, endoscopic, and PTCD interventions as well as pharmacological therapy, endoscopic PTCD stent drainage is the primary treatment selected by 80% of patients. Regrettably, the primary plastic and metal stent materials available have evident problems, including adherence to granulation tissue, biliary silt, and tumor invasion. In comparison, stents loaded with chemotherapy or Nonsteroidal Anti-inflammatory Drugs (NSAIDs) can inhibit tumor development or inflammation [4,6,11]. PTX is a natural substance frequently used in therapeutic applications [12–14].

In addition to metals, other materials, such as electrospinning and 3D printing, can be employed to fabricate stents [7]. Electrospinning utilizes electrohydrodynamics to create unique fibers. The utility model has a large surface area, high porosity, and involves a simple, low cost manufacturing process. Simultaneously, the polymer fiber membrane properties may be altered by incorporating nanoparticles, such as organic and inorganic components, enabling more precise control of drug and antibiotic release [10,15].

After charging with a high electric field, the polymer solution overcame the surface tension of the liquid. The nanofibers were collected on the receiver as the solution evaporated after being sprayed from the capillary nozzle. PTX was prepared by dissolving or dispersing it in PCL. When these stents were implanted, PTX was gradually released into the tumor tissue to achieve a long-term, relatively high concentration of local delivery; however, stents were degraded in the human body.

PTX is a frequently used anticancer drug that inhibits cell growth and activates the mitochondrial pathway for apoptotic molecular signaling [11,16]. PTX also exhibits antiangiogenic and antimetastatic properties. Furthermore, PTX is advantageous for locoregional cancer therapy because of its favorable pharmacokinetic properties (e.g., lipophilic and rapid cellular uptake) [16–18]. PTX-eluting covered bile stents, may represent a potential strategy for preventing occlusion due to tumor growth and further inhibiting tumor development. The biosafety of metal stents covering PTX has been reported in recent years [14,19]. Yuan et al. [20] compared the efficacy and safety of PTX-eluting metal stents (PECMS), metallic stents covered with a PTX-incorporated membrane (MSCPM), and conventional covered metal stents (CMS) in the treatment of malignant biliary obstruction. The findings revealed no significant changes in stent dysfunction, survival rate, biological safety, or stent stenosis caused by inward tumor growth, stent movement, or cholestasis. In terms of symptoms such as bile duct inflammation, patients with PECMS/MSCPM had a greater risk than those with CMS. Mohan et al. [21] showed that drug-eluting stents (DES) were more favorable in terms of stent opening and survival rates than those of self-expanding metal stents (SEMS) in patients with malignant bile obstruction (MBO). In the final two publications, research on PTX-eluting stents in animal tests did not describe concrete tumor growth. In our study, antitumor effects parameters in the transplanted tumor model included tumor volume, tumor volume rate, and mouse weight at different time points. During the trial period, the antitumor effect of the drug fiber membrane is described in further detail.

We used a PCL nanofiber loaded with PTX, which our laboratory provided at Ruijin Hospital, affiliated with Shanghai Jiao Tong University School of Medicine. The material used in this study possesses several advantageous properties, including excellent biocompatibility, high rate of drug loading, and mechanical properties. When combined with PTX, the copolymer exhibited additional antibacterial, bile stabilizing, and antitumor properties. Additionally, we evaluated the nanofibrous membrane drug loading rate and antitumor effects using *in vitro* and *in situ* experiments.

According to Figs. 2 and 3, a burst effect was observed in less than five days. In these two-line charts, the release percentage and quantity increased rapidly in the early stage but were relatively gentle in the late range. The release behaviors of the fiber and film membranes were similar, with similar release percentages at each time stage, eventually approaching 25%.

As shown in Fig. 3, the cumulative drug release percentage increased as the quantity increased. Consequently, the total sum of the releases increases simultaneously. Increasing the drug concentration may improve its release ability within a certain range. As an implant material, it enhances the cytotoxicity and therapeutic effects of local drug delivery.

Burst drug release was also monitored (Figs. 4 and 5). The release behavior varied between membranes containing varying amounts of the drug. The greater the drug quantity, the greater the ultimate release percentage. The total amount released ranged from 55 to 73% and the release behavior varied between the fibers and film. In the early stage, the film membranes released more drugs than the fiber membranes; however, the film membranes released almost no drugs during the late stage. The release curve progressed gradually, eventually reaching 48%. However, the drug release percentage of the fibers exceeded that of the films, eventually reaching 60%. In comparison to the pH 7.4 experiment, it can be concluded that the drug release rate and nanofibers amount were greater in an acidic environment such as the biliary duct.

Human bile is mildly alkaline under normal conditions, but an increase in the infiltration of acidic metabolites in local tumors lowers the pH, promoting the release of medication to boost the local effect. Therefore, we experimented both at pH 7.4 and 4.0 to simulate a biliary pH environment. The data demonstrated that the material was better released at low pH, implying that local tumors would infiltrate and create acid metabolites, resulting in a low pH condition that could be more favorable for drug release. The *in vitro* release studies conducted by Huang et al. [22] were similar to that of ours. Human bile was extracted in their experiment on the dissolution of biliary stones in flowing bile *in vitro*. However, membrane degradation was not investigated in that study. In future studies, we will focus on this issue and attempt to imitate the body's situation as much as possible.

After being placed in PBS, the PTX-mixed membranes floated, were suspended, and finally sank to the bottom, shrinking and expanding in the solution. Fig. 6b and c indicate that the greater the amount of drug, the greater the amount lost. Our study found that the highest quantity of loss occurred at 48%. This result indicates that small-fragment polymers are easily dissolved in the solution when membranes contain a high concentration of PTX. The fiber membranes' molecular weight loss was less than 28%, indicating that they behaved similarly to a typical surface corrosion model. We can define the loss of polymer structures as a decrease in polymer structures with increased drug content; however, the overall loss was less than 50%. In addition, when the molecular weight loss was less than 20%, the membranes performed similarly to the surface corrosion model. The molecular weight losses were less than 6% for the blank PCL electrospun fiber membranes, similar to the typical surface corrosion model.

To summarize these line charts and analyses, the membranes of different materials demonstrated varying degradation degrees. Regular drug-eluting membranes were used as the bulk-degrading model, whereas drug-mixed fiber membranes were used as the surface corrosion model. The degradation mechanism of most polymers is determined by the breakage of chemical bonds and the rate at which water molecules enter the polymers. When water molecules slowly penetrate the fiber bodies, the membrane acts as a surface corrosion barrier. A previous study discovered that PCL and drug-eluting electrospun fiber membranes made of PCL had low surface wettability, indicating that water molecules could not deeply penetrate the fiber bodies. Meanwhile, PLGA drug-eluting electrospun

fiber membranes exhibited the same degradation behavior, which could be exploited to extend the degradation time of the polymer and thus the release time of drugs such as anticancer and NSAIDs.

The drug-eluting electrospinning membrane demonstrated favorable release properties, exhibiting sustained release for a duration of one month along with a relatively smooth release profile. Moreover, in our mouse experiments, the PTX-releasing electrospinning membranes effectively suppressed the growth of tumor volume, thereby demonstrating significant *in vivo* anti-tumor efficacy.

Ethics approval and consent to participate

The experimental protocol was established according to the ethical guidelines of the Helsinki Declaration and was approved by the Ruijin Hospital, affiliated with the Shanghai Jiao Tong University Ethics Committee.

Consent for publication

Not Applicable.

Availability of data and material

The datasets generated and analyzed during the current study are not publicly available, as the data are being used in the next study, but are available from the corresponding author upon reasonable request.

Funding

This study was financially supported by the Shanghai Huangpu District Health Commission (Project No. HLQ202003).

The funding body had no role in the design of the study; collection, analysis, and interpretation of data; or preparation of the manuscript.

Authors' contributions

All authors lisPTX-releasing curve in pH 4.0 solutionhe paper.

Declaration of competing interest

The authors declare that they have no known competing financial interests or personal relationships that could have appeared to influence the work reported in this paper.

Acknowledgments

We thank Wenguo Cui for providing excellent research conditions and electrospun stents.

References

[1] C.D. Hair, et al., Future developments in biliary stenting [J], Clin. Exp. Gastroenterol. 6 (2013) 91–99, https://doi.org/10.2147/CEG.S34435.
[2] J.A. Tibble, et al., Role of endoscopic endoprostheses in proximal malignant biliary obstruction [J], J Hepatobiliary Pancreat Surg 8 (2) (2001) 118–123, https://doi.org/10.1007/s005340170033.
[3] W. Park, et al., Metallic stent mesh coated with silver nanoparticles suppresses stent-induced tissue hyperplasia and biliary sludge in the rabbit extrahepatic bile duct [J], Pharmaceutics 12 (6) (2020) 563, https://doi.org/10.3390/pharmaceutics12060563.
[4] A.I. Rezk, et al., A novel design of Tri-Layer membrane with controlled delivery of paclitaxel and anti-Biofilm effect for biliary stent applications [J], Nanomaterials 11 (2) (2021) 486, https://doi.org/10.3390/nano11020486.
[5] A.I. Rezk, et al., Drug release and kinetic models of anticancer drug (BTZ) from a pH-responsive alginate polydopamine hydrogel: towards cancer chemotherapy [J], Int. J. Biol. Macromol. 141 (2019) 388–400, https://doi.org/10.1016/j.ijbiomac.2019.09.013.
[6] J. Shatzel, et al., Drug eluting biliary stents to decrease stent failure rates: a review of the literature [J], World J. Gastrointest. Endosc. 8 (2) (2016) 77–85, https://doi.org/10.4253/wjge.v8.i2.77.
[7] B.S. Jang, et al., Advanced stent applications of material extrusion 3D printing for palliative treatment of unresectable malignant hilar biliary obstruction [J], Mater. Des. 195 (2020), 109005, https://doi.org/10.1016/j.matdes.2020.109005.
[8] T. Jiang, et al., Biomimetic Poly(Poly(ε-caprolactone)-Polytetrahydrofuran urethane) based nanofibers enhanced chondrogenic differentiation and cartilage regeneration [J], J. Biomed. Nanotechnol. 15 (5) (2019) 1005–1017, https://doi.org/10.1166/jbn.2019.2748.
[9] Y. Lv, et al., PLLA-gelatin composite fiber membranes incorporated with functionalized CeNPs as a sustainable wound dressing substitute promoting skin regeneration and scar remodeling [J], J. Mater. Chem. B 10 (7) (2022) 1116–1127, https://doi.org/10.1039/d1tb02677a.
[10] M.P. Arrieta, et al., Electrospinning of PCL-based Blends: Processing optimization for their scalable Production, J. Mater. 13 (17) (2020) 3853, https://doi.org/10.3390/ma13173853.
[11] M. Kalinowski, et al., Paclitaxel inhibits proliferation of cell lines responsible for metal stent obstruction: possible topical application in malignant bile duct obstructions [J], Invest. Radiol. 37 (7) (2002) 399–404, https://doi.org/10.1097/00004424-200207000-00007.
[12] F. Vogt, et al., Long-term assessment of a novel biodegradable paclitaxel-eluting coronary polylactide stent [J], Eur. Heart J. 25 (15) (2004) 1330–1340, https://doi.org/10.1016/j.ehj.2004.06.010.
[13] J.H. Shin, et al., Tissue hyperplasia: influence of a paclitaxel-eluting covered stent–preliminary study in a canine urethral model [J], Radiology 234 (2) (2005) 438–444, https://doi.org/10.1148/radiol.2342040006.

[14] D.K. Lee, et al., The effect on porcine bile duct of a metallic stent covered with a paclitaxel-incorporated membrane [J], Gastrointest. Endosc. 61 (2) (2005) 296–301, https://doi.org/10.1016/s0016-5107(04)02570-2.
[15] M. Rabionet, et al., Electrospinning PCL scaffolds manufacture for three-dimensional Breast cancer cell culture, J]. Polymers (Basel) 9 (8) (2017) 328, https://doi.org/10.3390/polym9080328.
[16] F.Y. Alqahtani, et al., Alkahtani and BT AlQuadeib. Paclitaxel [J], Profiles Drug Subst. Excipients Relat. Methodol. 44 (2019) 205–238, https://doi.org/10.1016/bs.podrm.2018.11.001.
[17] E. Gavathiotis, et al., BAX activation is initiated at a novel interaction site [J], Nature 455 (7216) (2008) 1076–1081, https://doi.org/10.1038/nature07396.
[18] I. Noh, et al., Co-delivery of paclitaxel and gemcitabine via CD44-targeting nanocarriers as a prodrug with synergistic antitumor activity against human biliary cancer [J], Biomaterials 53 (2015) 763–774, https://doi.org/10.1016/j.biomaterials.2015.03.006.
[19] S.I. Jang, et al., Safety evaluation of paclitaxel-eluting biliary metal stent with sodium caprate in porcine biliary tract [J], Gut Liver 13 (4) (2019) 471–478, https://doi.org/10.5009/gnl18454.
[20] T. Yuan, et al., Efficacy and safety evaluation of paclitaxel-loaded metal stents in patients with malignant biliary obstructions [J], Eur. J. Surg. Oncol. 45 (5) (2019) 816–819, https://doi.org/10.1016/j.ejso.2018.10.533.
[21] B.P. Mohan, et al., Drug eluting versus covered metal stents in malignant biliary strictures-is there a clinical Benefit?: a systematic review and meta-analysis [J], J. Clin. Gastroenterol. 55 (3) (2021) 271–277, https://doi.org/10.1097/MCG.0000000000001377.
[22] C. Huang, et al., Drug-eluting fully covered self-expanding metal stent for dissolution of bile duct stones in vitro [J], World J. Gastroenterol. 25 (26) (2019) 3370–3379, https://doi.org/10.3748/wjg.v25.i26.3370.